J. exp. Biol. **149**, 469–489 (1990)
Printed in Great Britain © *The Company of Biologists Limited 1990*

AERODYNAMICS OF GLIDING FLIGHT IN A HARRIS' HAWK, *PARABUTEO UNICINCTUS*

BY VANCE A. TUCKER AND CARLTON HEINE
Department of Zoology, Duke University, Durham, NC 27706, USA

Accepted 31 October 1989

Summary

1. A Harris' hawk with a mass of 0.702 kg and a maximum wing span of 1.02 m glided freely in a wind tunnel at air speeds between 6.1 and 16.2 $m\,s^{-1}$. The glide angle varied from 8.5° at the slowest speed to a minimum of 5° at speeds between 8.0 and 14.7 $m\,s^{-1}$. The maximum ratio of lift to drag was 10.9 and the minimum sinking speed was 0.81 $m\,s^{-1}$.

2. Wing span decreased when either air speed or glide angle increased. Wing area was a parabolic function of wing span.

3. Lift and profile drag coefficients of the wings fell in a polar area similar to that for a laggar falcon (*Falco jugger*) and a black vulture (*Coragyps atratus*). A single polar curve relating lift coefficients to minimum profile drag coefficients can predict the maximum gliding performance of all three birds when used with a mathematical model for gliding flight.

4. The parasite drag values that have been used with the model are probably too high. Thus, the profile drag coefficients determined from the polar curve mentioned above are too low, and the predicted wing spans for gliding at maximum performance are too large. The predicted curve for maximum gliding performance is relatively unaffected.

5. The maximum lift coefficient for the Harris' hawk in the wind tunnel was 1.6. This value is probably less than the maximum attainable, since the hawk's wings never appeared to stall. The best estimate of the minimum profile drag coefficient is 0.026 at a lift coefficient of 0.60.

Introduction

Soaring birds take advantage of air currents to remain aloft for long periods without flapping their wings. In still air, however, they glide along a downward-inclined flight path and eventually come to earth. A bird's aerodynamic characteristics determine how far and for how long it can glide, and how successfully it can soar in moving air. Pennycuick (1975, 1989) reviewed the aerodynamic characteristics of soaring birds, the motions of the air through which they glide and the manoeuvres that they use to stay aloft and move with respect to the ground.

Birds can optimize their aerodynamic characteristics by changing their wing

Key words: bird flight, glide angle, gliding performance, lift coefficient, polar curve, profile drag, sinking speed, wind tunnel.

spans and wing areas in flight. Tucker (1987, 1988) discusses the aerodynamic consequences of this behaviour and describes a mathematical model that predicts the maximum gliding performance of a bird at equilibrium – i.e. when both the bird and the air through which it moves have constant velocities relative to the earth. The model uses empirical data from a laggar falcon (Tucker and Parrott, 1970) and a black vulture (Parrott, 1970) gliding freely in a wind tunnel. Surprisingly, the wings of these birds have similar aerodynamic characteristics in spite of the fact that the falcon wings are long with pointed tips while the vulture wings are broad with square tips.

In this paper, we report the aerodynamic characteristics of a Harris' hawk *Parabuteo unicinctus* Temminck (described in Bednarz, 1988; Clark, 1987) gliding at equilibrium in a wind tunnel. This bird is native to the southwestern United States and resembles small hawks of the genus *Buteo*. Harris' hawk wings have rounded tips that are intermediate in shape between those of the falcon and the vulture. We wanted to determine (1) whether the aerodynamic characteristics of Harris' hawk wings are similar to those of the falcon and the vulture, and (2) how well the gliding performance of the hawk conformed to the predictions of the mathematical model.

Theory

A bird gliding at equilibrium moves at constant air speed V along a path inclined downwards at angle θ to horizontal (the glide angle, Fig. 1) and sinks steadily through the air with sinking speed V_s:

$$V_s = V\sin\theta. \quad (1)$$

If the bird glides in a tilted, ideal wind tunnel, it remains motionless relative to the earth when the air flows upwards through the tunnel at speed V and angle θ. In an ideal tunnel, the air flow past the bird and the forces on it are identical to those in free air. Actual tunnels differ from ideal ones because of boundary effects (see Materials and methods).

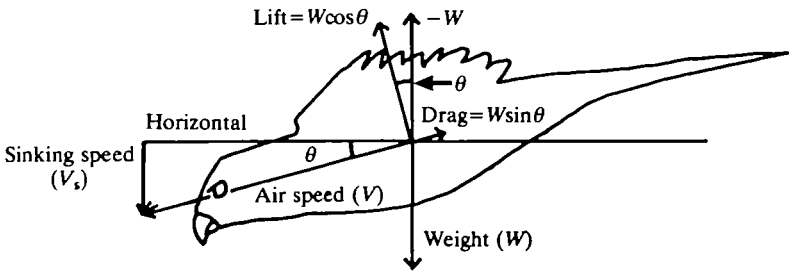

Fig. 1. Forces and velocities during equilibrium gliding. The glide path is inclined at glide angle θ to the horizontal. Lift and drag are parallel and perpendicular, respectively, to the glide path. Air speed (V) is parallel to the glide path, and sinking speed (V_s) is vertical and downwards.

Pennycuick (1968) published the first study of a bird gliding freely in a tilted wind tunnel. The following theoretical treatment derives from that paper and others mentioned in Tucker (1987). Additional information may be found in aerodynamic texts and in Pennycuick (1989).

The aerodynamic force on a bird gliding at equilibrium points vertically upwards and is equal in magnitude to the bird's weight (W), which is the product of mass and gravitational acceleration (Fig. 1). The force has two components: total drag (D), parallel to the flight path and given by:

$$D = W\sin\theta, \tag{2}$$

and lift (L), perpendicular to the flight path and given by:

$$L = W\cos\theta. \tag{3}$$

We make the conventional assumption that only the wings produce significant lift. This assumption is reasonable for the Harris' hawk, which did not spread its tail widely at the speeds used in this study.

The lift and drag components depend on the bird's size and air speed. We shall describe these components with two related quantities that are less dependent on size and air speed: dimensionless force coefficients and equivalent flat plate areas.

Force coefficients

A force coefficient is the ratio of the aerodynamic force (or its component) on an object to the theoretical aerodynamic force on a flat plate of area S held perpendicular to the air flow. S is an area on the object chosen to make the force coefficient relatively independent of the object's size and speed. For a wing (the term includes both left and right wings), S is the maximum projected area of the wing at a given span, including the part covered by the body. The lift and drag coefficients for the wing in air of density ρ are:

$$C_L = L/(0.5\rho SV^2), \tag{4}$$

and

$$C_D = D/(0.5\rho SV^2). \tag{5}$$

Force coefficients vary with the orientation of the object and with Reynolds number (Re):

$$Re = \rho dV/\mu, \tag{6}$$

where d is a reference length of the object and μ is the viscosity of the air. The ratio ρ/μ (the reciprocal of kinematic viscosity) has the value 68 436 s m^{-2} for air at sea level in the US standard atmosphere (von Mises, 1959). The Reynolds number of the hawk in this study varied between 78 000 and 208 000 for a reference length equal to the mean chord (c') of the wing at maximum span (b_{max}):

$$c' = S_{max}/b_{max}. \tag{7}$$

S_{max}, the maximum wing area, occurs at b_{max}. The aspect ratio of the wing is b_{max}/c'.

Equivalent flat plate area

The equivalent flat plate area (S_{fp}) is the ratio of an aerodynamic force (drag in this study) on an object to the theoretical pressure on a flat plate held perpendicular to the air flow:

$$S_{fp} = D/(0.5\rho V^2) . \quad (8)$$

This ratio equals the area of a flat plate that has the same drag as the object itself. It remains relatively constant for a given object as V changes. We use it to calculate the drag of the hawk's body at different speeds.

Drag

We divide the total drag (D) on the bird into three components: induced drag (D_i), parasite drag (D_{par}) and profile drag (D_{pr}):

$$D = D_i + D_{par} + D_{pr} . \quad (9)$$

Induced drag

Induced drag (D_i) arises when the wings produce lift:

$$D_i = 2kL^2/(\pi\rho b^2 V^2) , \quad (10)$$

where k, the induced drag factor, has the value 1.1, π is the ratio of the circumference to the diameter of a circle and b is wing span. k may change with wing span, but there are insufficient data to account for such changes. Tucker (1987) gives more information on k and the effect of changes in its value.

Parasite drag

Parasite drag (D_{par}) is the drag on the bird exclusive of the drag on the wings. We subdivide it into two components: the minimum drag ($D_{par,B}$) on a wingless bird body at a given speed, and any extra drag (the residual drag) that arises when the bird does not hold its body in the minimum drag configuration. [Tucker (1990) worked with an isolated bird body and used the symbol D_B for $D_{par,B}$.] We calculate $D_{par,B}$ from an equivalent flat plate area given by an empirical equation for wingless bird bodies ($S_{fp,B}$) (Tucker, 1973):

$$S_{fp,B} = 0.00334m^{0.660} , \quad (11)$$

where m is the body mass of the intact bird. This equation probably overestimates $S_{fp,B}$ for the Harris' hawk (Tucker, 1990), but we use it for consistency with a theoretical treatment of gliding flight (Tucker, 1987).

Residual drag arises when the bird extends its feet, lowers or spreads its tail or yaws – i.e. glides with the long axis of its wings not perpendicular to the direction of air flow. In addition, the air flow around the body of an intact bird differs from that around an isolated body because of the wings. We assume that the drag of the intact bird is the sum of the drags of the wingless body and the bodyless wings. This assumption is plausible but not necessarily true. When these parts are joined, each

has less surface area, which reduces drag. However, the different air flow over the joined parts may add interference drag. Residual drag includes the net effect, which may or may not be negligible (Hoerner, 1965). We discuss residual drag but assume that it is zero for most calculations.

Profile drag

Profile drag (D_{pr}) is the drag on the wings due to skin friction and pressure differences. We determine it by difference:

$$D_{pr} = D - D_i - D_{par} . \quad (12)$$

The profile drag coefficient is given by:

$$C_{D,pr} = D_{pr}/(0.5\rho SV^2) . \quad (13)$$

$C_{D,pr}$ varies with C_L, and a polar diagram (for example, Fig. 5) with $C_{D,pr}$ on the horizontal axis shows the relationship between the two. The data for gliding birds fall in a polar area because bird wings have adjustable span, aerofoil sections and degree of twist from base to tip at a given air speed (Tucker, 1987). In contrast, the data for conventional rigid wings fall on a single polar curve. The left-hand boundary of the polar area is the polar curve for minimum drag.

The polar curves for rigid wings with bird-like aerofoils shift horizontally as Re changes between 75 000 and 10^6. We calculated the shift from the relationship:

$$F = 1.21 - 0.226(Re \times 10^{-5}) + 0.0151(Re \times 10^{-5})^2 , \quad (14)$$

where F is the ratio $C_{D,pr}/(C_{D,pr}$ at $Re \times 10^{-5}=1)$ (Tucker, 1987). We corrected all $C_{D,pr}$ values in this paper to an Re of 10^5.

Theoretical maximum performance curve

A gliding bird can achieve a range of sinking speeds at each air speed by varying its wing shape and span (Tucker, 1987). The minimum V_s values attainable at each speed define the bird's maximum performance curve (for example, Fig. 8). At maximum performance, the bird minimizes drag, as can be seen by combining equations 1 and 2:

$$V_s = DV/W . \quad (15)$$

A bird can adjust its wing span (b) to minimize drag because, for a given $C_{D,pr}$, induced drag and profile drag change in opposite directions when wing span changes. However, $C_{D,pr}$ itself changes with wing span (Tucker, 1987). The optimum wing span and the minimum V_s at a particular speed depend on the relationship between S and b, and on the polar curve for minimum drag.

Tucker (1987) describes a mathematical model for calculating the maximum performance curves for gliding birds when S is a linear function of b, and therefore the derivative dS/db has a constant value (C_3). In the present study, S is a

parabolic function of b, so we use Tucker's (1987) equation 30 in a more general form that applies when S is any differentiable function of b:

$$\frac{dD}{db} = -2k_3L^2/(b^3V^2) + k_4\frac{dS}{db}\{C_0V^2 - C_2[k_6L/(VS)]^2\}. \quad (16)$$

Materials and methods

Wind tunnel

The wind tunnel (described by Tucker and Parrott, 1970) had a closed, rectangular working section 1.85 m long, 1.37 m wide and 1.07 m high with Plexiglas sides and roof. A steel rib 5.6 cm wide ran from front to back along the midline of the roof. Hardware cloth screens closed the upstream and downstream ends of the working section. A variable-speed fan powered the wind tunnel, and the entire tunnel could tilt a maximum of 8.5° around a horizontal axis perpendicular to the direction of air flow.

We determined air speed in the working section with a pitot-static tube connected to an electronic manometer (Datametrics Barocel 1174) calibrated with a water manometer. The pitot tube measured the dynamic pressure (q), which is related to air speed:

$$V = (2q/\rho)^{1/2}. \quad (17)$$

Air speeds in this study are given for the US standard atmosphere at sea level (density=1.23 kg m^{-3}, von Mises, 1959). We regulated air speed by adjusting the speed of the fan while observing a digital meter. The meter was referenced to a crystal clock and showed the time required for each rotation of the fan. The spatial variation in air speed in the region where the bird flew was 0.2 m s^{-1}.

We measured the vertical angle of the air flow direction in the working section with a yawmeter (similar to the one illustrated in Fig. 4.48a of Gorlin and Slezinger, 1966) connected to the Barocel. This angle, relative to horizontal, is the glide angle (θ). We rotated the yawmeter around its longitudinal axis to determine when it was parallel to the air flow. The glide angle varied by 0.25° in the region of the working section where the hawk flew for the range of speeds and tunnel tilts used in this study.

Harris' hawk and training

We used a tame male hawk (provided by the US Fish and Wildlife Service) that had been hatched and raised in captivity. On each tarsus, the hawk wore leather cuffs with brass eyelets to which jesses could be attached. The cuffs protruded 1.5 cm from each leg. We trained the hawk to fly to a leather glove for food (dead mice) and perch on it while eating. During the experiments, the mass of the hawk varied from 0.702 kg by less than 1%.

We trained the hawk to fly in the wind tunnel by working with it every day for two, 20-min sessions. At first, one of us entered the tunnel with the hawk perched

on his gloved hand. The hawk spread its wings in the wind but clung to the glove. The trainer gently unhooked the bird from the glove and tossed it into the air, where it flew for a few seconds before landing on the glove. We encouraged the bird to fly longer by tossing it into the air again when it tried to land. After 2 weeks, it would glide for more than 10 s.

At this point, the trainer moved outside the wind tunnel and left the hawk inside, perched on the glove on the floor. The trainer reached through the door of the working section with a broom handle 1.5 m long, which he inserted into the glove. He raised the bird from the floor, turned on the tunnel, shook the bird into the air and returned the handle and glove to the floor. The bird would land only on the glove, and the trainer encouraged it to fly for increasing periods by manipulating the glove with the handle. He shook the glove when the bird tried to land after a short flight, but held the glove up for the bird to land on after a flight of acceptable duration. After a month, the hawk would fly for several minutes until the trainer opened the door to the working section, reached in and raised the glove for a landing. The hawk continued to behave in this fashion as long as we had it (4 months), even without daily training.

Photography and planimetry

A 35-mm motor-driven camera mounted on the tunnel 1.37 m above the Plexiglas roof of the working section was used to photograph the hawk from above. An electronic flash mounted inside the working section provided illumination. The axis of the camera's 35 mm lens intersected the longitudinal midline of the working section and was perpendicular to the roof.

We traced each photographic negative after projecting it onto a piece of paper with an enlarger. We completed the perimeter of the wings on the tracing by drawing in (1) a straight line that joined the points where the leading edges of the wings met the body, (2) a similar straight line for the trailing edges and (3) the parts of the leading and trailing edges that were obscured by the rib on the roof of the working section. We then measured wing area by running the stylus of a planimeter around the perimeter of the wing, including the indentations between the feathers. We also measured the wing span (the maximum distance between corresponding points on each wing tip) on each tracing and the basal chord of the wings. The basal chord is the shortest distance between the leading and trailing edges of the left wing on the part of the wing between the distal end of the humerus and the body. We measured the basal chord on the right wing when the left wing was obscured.

We determined the actual length of the basal chord by photographing the gliding hawk as it carried a paper streamer of known length (0.196 m). The streamer attached to a paper collar around the bird's neck and ran down the midline of the back. The mean basal chord length was 0.184 m (relative standard deviation=2.3 % of the mean value, 23 measurements) and did not change as wing span varied between 55 % and 100 % of maximum.

The accuracy of the photographic method depends on the accuracy of (1) tracing

and planimetry, and (2) the amount of distortion in the optical systems of the camera and enlarger. We evaluated errors from these sources as follows. (1) We traced and planimetered one photograph of the hawk five times. The relative standard deviations of the span and area were 0.981 % and 1.52 %, respectively, of the mean values. (2) We evaluated optical distortion by tracing and planimetering a photograph of six square plates, 0.305 m on each side, laid out on the floor of the working section and arranged so that their images appeared in the centre and along the edges of the negative. The side lengths and areas of the plates in the tracing had relative standard deviations of 0.532 % and 0.627 %, respectively, relative to the mean values. Since these percentages include tracing and planimetry errors, they overstate the errors due to distortion. The mean side length and area of the plates, as determined by the photographic method, were within 0.1 % and 0.5 %, respectively, of the actual dimensions of the plates.

We ignored any effect on wing area due to the plane of the wings not being perpendicular to the axis of the camera lens. Any error from this source is small, since it is a function of the cosine of the angle (β) between the plane of the wings and a perpendicular to the lens axis. The camera tilted with the wind tunnel, so β varied only with the geometric angle of attack of the wings, the angle of bank and the angle of the wing dihedral. All these angles (estimated by eye) were less than 15°, and the cosine of β decreases by only 3 % as β changes from 0 to 15°.

Experimental protocol

We photographed the hawk as it was gliding at equilibrium at predetermined speeds and glide angles. Our criterion for equilibrium was that the hawk remained 'motionless' for at least 1 s. Motionless means that the wings did not flap, and the hawk's body did not move up or down, forward or back more than 2 cm (judged by eye) during the second.

We changed the glide angle in steps of 0.5° or more. The 'minimum glide angle' is the shallowest angle at which the hawk would glide at equilibrium. After finding the minimum glide angle, we tried reducing it by 0.25°, but the hawk would not glide at equilibrium at the shallower angle.

Data reduction and accuracy

We calculated various quantities with the equations given in the Theory section. We corrected for wind tunnel boundary effects (Pope and Harper, 1966; Tucker and Parrott, 1970) by adding the following term to total drag:

$$\rho(SC_{\mathrm{L}}V)^2/(16C),$$

where C is the cross-sectional area (1.5 m^2) of the wind tunnel working section. We calculated sinking speed from the corrected drag and equation 15.

Table 1 shows the accuracy of our basic measurements.

Table 1. *Accuracy of measurements*

Quantity	Relative bias (%)	Relative imprecision (%)
Pressure	0.07	0.46
Time	0.01	0.1
Air speed	0.035	0.23
Glide angle	4.0	1.0
Wing span	0.2	2.5
Wing area	0.7	4.8

Bias is the difference between the mean value (M) of repeated measurements of a quantity and the true mean, and imprecision is the standard deviation of repeated measurements of a quantity (Eisenhart, 1968).

Relative bias and imprecision are expressed as percentages of the maximum values of M reported in this study.

When necessary, we used propagation of error formulae (Ku, 1969) to calculate bias and imprecision.

Results

Behaviour

The hawk usually followed a basic flight pattern in the top half of the working section. It glided to the front of the working section, drifted to the back, flapped its wings a few times and gained a position nearly at the centre, then started gliding again. It modified the timing of this pattern, depending on speed and glide angle. Sometimes it lowered its legs into the air stream or glided with the long axis of its wings yawed at an angle up to 25° from the transverse axis of the wind tunnel.

At glide angles steeper than minimum, the gliding part of the basic cycle was relatively long (up to 10 s). The hawk often glided at equilibrium, remaining motionless for a second or more. It sometimes held its wings yawed and, at speeds less than $10\,m\,s^{-1}$, often lowered its legs into the air stream. The slower the speed and the steeper the angle the more it extended its legs. In the extreme, it exposed the feathered tibial regions, the tarsi and the spread toes to the air stream. At higher speeds and shallower angles, the hawk progressively retracted its legs; first clenching its toes, then raising the tibial regions and finally tucking its tarsi and feet under its tail.

At minimum glide angles, the gliding part of the basic pattern was short (about 5 s). When the hawk glided at equilibrium, it kept its feet tucked up under its tail (except at the slowest speed of $6.1\,m\,s^{-1}$) and its wings unyawed. At $6.1\,m\,s^{-1}$, the hawk lowered its tarsi and clenched feet into the air stream. We usually had to watch for a minute or more before we saw an episode of equilibrium gliding.

The hawk soon landed if we reduced the air speed below $6.1\,m\,s^{-1}$. It spread its tail widely at these low speeds, the only time that we saw this behaviour.

Wing span at different speeds and glide angles

The hawk varied its wing span as its glide angle and speed changed. For a given

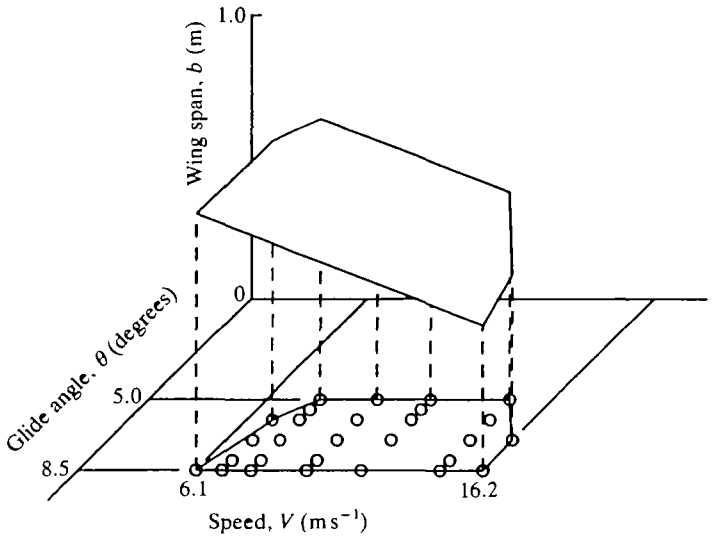

Fig. 2. Three-dimensional surface showing the relationship between speed (V), glide angle (θ) and wing span (b) for a Harris' hawk gliding at equilibrium. Dashed, vertical lines connect the minimum glide angle at each speed to its projection on the horizontal plane for a wing span of zero. Additional points on the horizontal plane show other combinations of speeds and angles at which wing span was measured. Lines on the horizontal plane show maximum and minimum speeds and angles.

glide angle, the wing span decreased as the speed increased and, for a given speed, wing span decreased as the glide angle increased. A plane (Fig. 2) fitted by least-squares (Snedecor and Cochran, 1980) adequately described the data:

$$b = 1.538 - 0.0389V - 0.0469\theta, \quad (18)$$

(N=153, standard deviation of b around the plane=0.0586 m). The projection of the data onto the V,θ plane shows the combinations of V and θ at which we set the wind tunnel.

The mean measured values of b, θ and total drag for the hawk gliding at the minimum glide angle at each speed (Table 2) comprise the basic data for many of the computations in this study.

Table 2. *Basic data for the Harris' hawk at minimum glide angles*

Speed ($m s^{-1}$)	Glide angle (degrees)	Wing span (m)	Total drag (N)
6.1	8.5	1.012	1.188
7.0	6.0	1.018	0.850
8.0	5.0	0.979	0.700
10.0	5.0	0.876	0.664
11.9	5.0	0.801	0.646
14.7	5.0	0.754	0.630
16.2	7.0	0.630	0.864

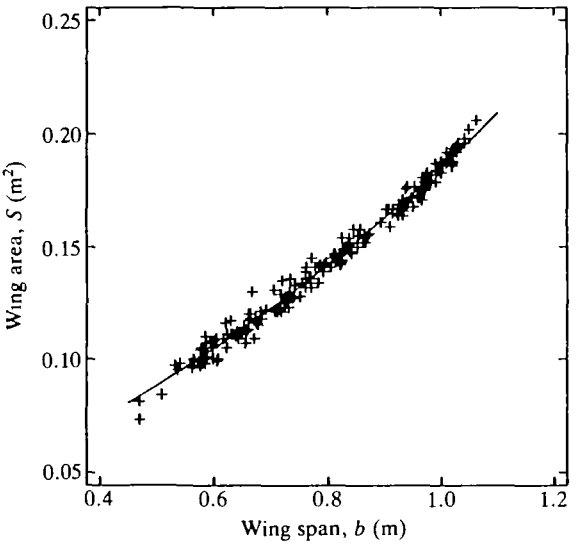

Fig. 3. The relationship between wing span and wing area for a Harris' hawk gliding in a wind tunnel.

Wing area and wing span

Wing area increased with wing span along a parabolic curve (Fig. 3) fitted by least squares:

$$S = 0.0278 + 0.0841b + 0.0736b^2 \quad (19)$$

(N=183, standard deviation around the curve=0.00375 m^2).

The maximum wing span and area occurred when the bird was gliding at 7.0 $m\,s^{-1}$ with a glide angle of 6°. The mean wing span of seven measurements at this speed and angle was 1.018±0.0237 m (S.D.) and the mean wing area was 0.191±0.0076 m^2 (S.D.).

The shape of the wings changed markedly as the wing span changed. At maximum span, the separated primary feathers formed rounded wing tips (Fig. 4). At shorter spans, the primaries formed pointed, swept-back tips.

Lift and profile drag coefficients

C_L and $C_{D,pr}$ values fell in a polar area (Fig. 5) (terminology from Tucker, 1987). The left-hand boundary of the polar area is the polar curve for minimum drag (Fig. 6). We found this curve by fitting a parabola (by least squares) to the mean values of C_L and $C_{D,pr}$ at minimum glide angles:

$$C_{D,pr} = 0.0290 - 0.0782C_L + 0.0763C_L^2 \quad (20)$$

(N=7, standard deviation of points around line=0.00399). The C_L and $C_{D,pr}$ values within the polar area are scattered around polar curves for constant speed (Fig. 6).

Discussion

Lift and profile drag coefficients

The C_L and $C_{D,pr}$ values for the hawk wing are similar to those measured in two other raptorial birds, a laggar falcon (*Falco jugger*, similar to a peregrine falcon) and a black vulture (*Coragyps atratus*), gliding in a wind tunnel (Tucker, 1987). We

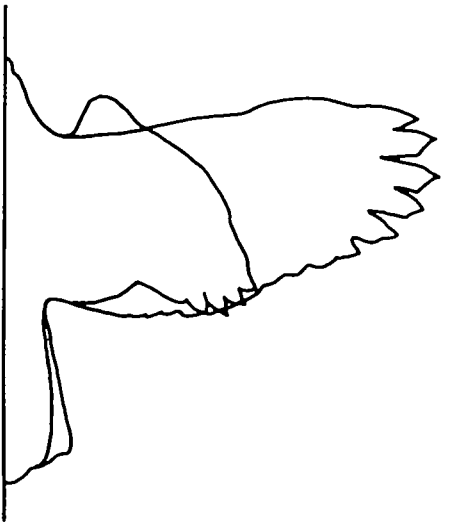

Fig. 4. Shapes of extended and flexed wings of a Harris' hawk gliding at $7.0\,m\,s^{-1}$ and a glide angle of 6.0° (extended), and $16.2\,m\,s^{-1}$ and a glide angle of 8.5° (flexed). The tail is wider with extended wings.

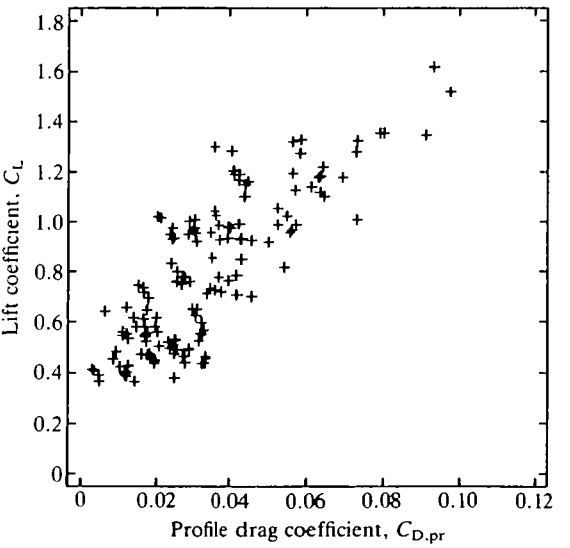

Fig. 5. Polar area for the wings of a Harris' hawk gliding at equilibrium at the speeds and angles shown in Fig. 2.

shall refer to these two birds and the hawk in the following discussion as 'the hawk', 'the falcon' and 'the vulture'. The data for all three fall in polar areas (Fig. 7).

Although the polar curve for minimum drag (the left-hand boundary of the

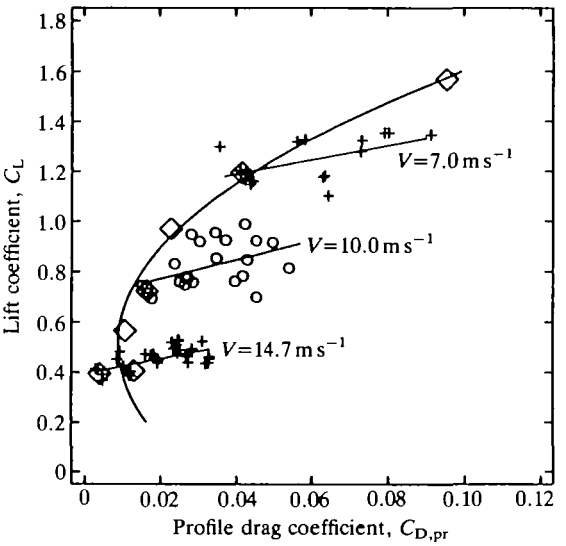

Fig. 6. Polar curves for the wings of a Harris' hawk. The polar curve for minimum drag (curved line) is fitted to mean values (diamonds) of C_L and $C_{D,pr}$ at minimum glide angles. Only three polar curves for constant speed (straight lines) are shown to avoid cluttering the diagram. Curves for other speeds are similar.

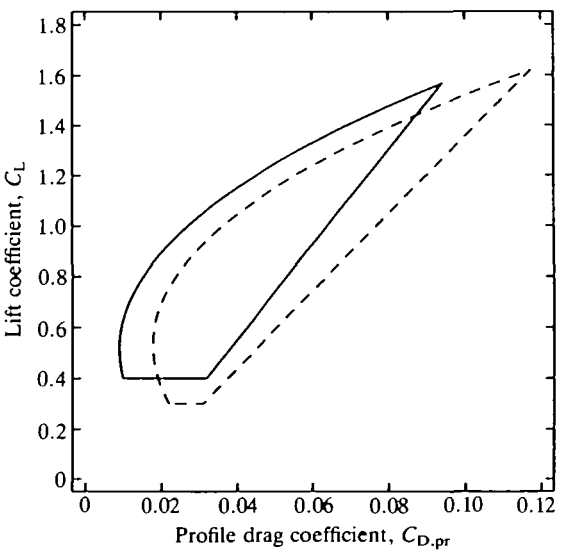

Fig. 7. The polar area for the Harris' hawk (solid lines) superimposed on the polar area for the laggar falcon and the black vulture (dashed lines).

polar area) for the hawk is to the left of that for the falcon and the vulture, the curves have strikingly similar shapes, considering the differences between these three birds. The falcon and the hawk are about the same weight, but the vulture weighs three times as much. At maximum span, the hawk wings have rounded tips with separated primary feathers and an aspect ratio of 5.5. The vulture wings have square tips with separated primaries (aspect ratio=5.6), and the falcon wings have pointed tips without separated primaries (aspect ratio=7.7).

The right-hand boundary of the polar area is the polar curve for maximum drag (Tucker, 1988). However, the $C_{D,pr}$ values in this study are not maxima for two reasons. First, maximum profile drag coefficients occur when the wings stall – for example, at the low air speeds and high sinking speeds associated with landing (Tucker, 1988). In a stall, the feathers on the tops of the wings lift and flutter in the air stream. The hawk's wing feathers sometimes did this when the bird clung to the glove and spread its wings during training, but never during free flight. When the air speed decreased enough to cause a stall, the hawk either landed or began flapping.

Second, some profile drag coefficients in Fig. 5 are probably too high because of residual drag. When the hawk glided at low speeds and at angles steeper than minimum, it sometimes extended its legs or yawed. These manoeuvres add residual drag to body drag. Residual drag appears as profile drag in this study, since profile drag is calculated by difference (equation 12).

Although we did not measure residual drag, we can estimate it from measurements on the body of a Rüppell's griffon vulture (*Gyps rüppellii*) with extended legs (Pennycuick, 1971). The residual drag of the partly extended legs (the tarsi and the feet were exposed to the air stream) was 0.66 times body drag. The residual drag of the fully extended legs (the tibiae were exposed) was 2.18 times body drag. From these figures, we can estimate the equivalent flat plate area ($S_{fp,r}$) of residual drag for the extended legs and, hence, the change in $C_{D,pr}$, since $\Delta C_{D,pr}=-S_{fp,r}/S$.

At the minimum glide angle and a speed of $6.1\,m\,s^{-1}$, the hawk partly extended its legs. The residual drag of the legs under these conditions adds 0.011 to $C_{D,pr}$ at $C_L=1.6$. The hawk sometimes fully extended its legs at a glide angle of 8.5° and a speed of $7\,m\,s^{-1}$, thereby adding 0.037 to $C_{D,pr}$ – nearly enough to account for the entire change in $C_{D,pr}$ along the polar curve for constant speed (Fig. 6). The hawk sometimes partly extended its legs at a glide angle of 8.5° and a speed of $10\,m\,s^{-1}$, adding 0.0136 to $C_{D,pr}$. At higher speeds, the hawk seldom extended its legs.

Any increase in induced drag above that calculated from equation 10 will also appear as profile drag. Gliding birds may increase induced drag for a given wing span by twisting the wings to increase lift at the wing tips. This change in the lift distribution increases the induced drag factor (Pennycuick, 1971; Tucker, 1987).

Maximum C_L

The maximum C_L for the hawk was 1.6, compared with 1.6 for the falcon and 1.1 for the vulture. These values are probably less than the maximum C_L

attainable, which occurs when the wings begin to stall. None of these birds showed signs of stalling. In contrast, landing white-backed vultures (*Gyps africanus*) with stalled wings appeared to have a maximum C_L of 2.2 (Tucker, 1988).

Variation of span with glide angle

There is just one wing span at a given speed that will minimize profile and induced drag, and hence glide angle. At steeper angles, the bird maintains its speed by increasing drag, which it may accomplish by either increasing or decreasing wing span (Tucker, 1987). Consequently, the wing span should be less variable when birds are gliding near the minimum glide angle rather than at steeper angles.

We measured variability of wing span at different glide angles by computing the standard deviation of wing span around the regression line for wing span on speed. We used only speeds between 8.0 and 14.7 $m\,s^{-1}$, since the hawk could attain the minimum glide angle of 5° only over this range. As expected from theory, the variation is least at the minimum glide angle (Fig. 8).

Comparison with the maximum performance model

The maximum performance model uses a polar curve for minimum drag (PCMD) fitted to data for the falcon and the vulture corrected to an *Re* of 10^5 (Tucker, 1987). Since this curve is to the right of the curve for the hawk (Fig. 7), the model overestimates the minimum sinking speeds of the hawk (Fig. 9). (The PCMD should not be confused with the term 'glide polar' which sometimes is used to describe a curve relating sinking speed to air speed.)

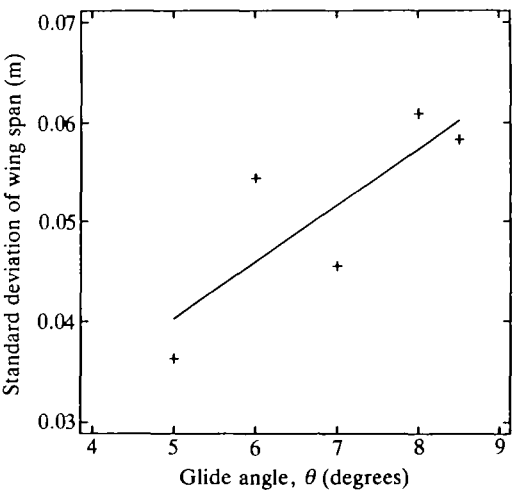

Fig. 8. The variation of wing span with speed of a Harris' hawk gliding at different glide angles. Variation is measured by the standard deviation of the wing span around the regression line of span on speed at each glide angle. Each standard deviation is based on between 18 and 31 wing span measurements.

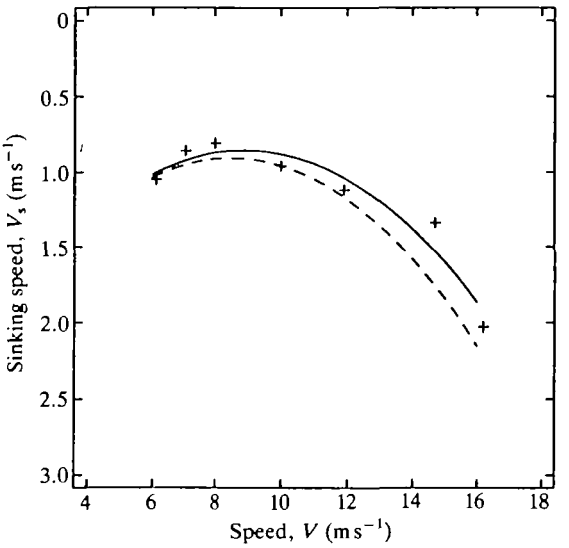

Fig. 9. A maximum performance curve (solid line) fitted to measured data (crosses) for the Harris' hawk superimposed on the theoretical curve (dashed line) calculated from the maximum performance model. The model uses the polar curve for minimum drag fitted to data for the falcon and the vulture (Tucker, 1987).

The model may be modified to use a new PCMD fitted to mean data for the hawk, the falcon and the vulture:

$$C_{D,pr} = 0.0371 - 0.0835C_L + 0.0793C_L^2 \quad (21)$$

(N=21, standard deviation around curve=0.00060). The modified model predicts the maximum performance of all three birds with reasonable accuracy (Fig. 10 and Table 3).

However, equation 21 should be used with caution for purposes other than predicting maximum performance curves, because it is calculated (equation 12) from an equivalent flat plate area for parasite drag ($S_{fp,B}$, equation 11) that probably is too high (Tucker, 1990). If so, it yields profile drag coefficients that are too low.

Fig. 11 shows how the PCMD for the Harris' hawk depends on $S_{fp,B}$. The dashed curve duplicates that in Fig. 6 and is based on an $S_{fp,B}$ value of 0.00264 m^2 from equation 11. The solid curve is based on an S_{fp} value of 0.00120 m^2, estimated from data on a peregrine falcon of similar size and shape with a body drag coefficient of 0.18 (Tucker, 1990). The equation of the solid curve is:

$$C_{D,pr} = 0.0522 - 0.1032C_L + 0.0858C_L^2 \quad (22)$$

(N=7, standard deviation of points around line=0.00485). This equation gives a minimum value for $C_{D,pr}$ of 0.026 when C_L is 0.60.

The performance curve predicted by the maximum performance model is relatively insensitive to erroneous $S_{fp,B}$ values if one uses the same $S_{fp,B}$ value to

calculate both the PCMD and the performance curve (Fig. 12). If parasite drag is too high, profile drag is too low. Both variables appear in the maximum performance model, and the two errors partially compensate for one another.

In contrast, the wing spans predicted by the maximum performance model are relatively sensitive to erroneous $S_{fp,B}$ values. When $S_{fp,B}$ is too high, so is the

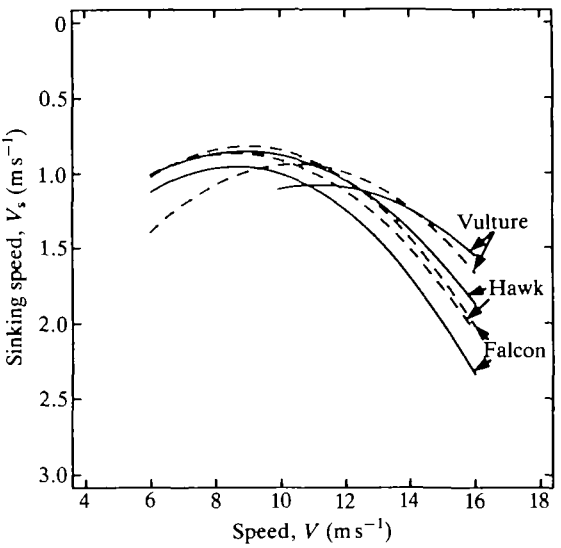

Fig. 10. The measured maximum performance curves (solid lines) for the Harris' hawk, the falcon and the vulture superimposed on theoretical curves (dashed lines) calculated from the maximum performance model. The model uses the polar curve for minimum drag fitted to data for all three birds (equation 21). Table 3 gives the equations for the curves.

Table 3. *Coefficients for maximum gliding performance**

	a_0	a_1	a_2
Harris' hawk			
Measured	2.39	−0.348	0.0197
Theoretical	2.43	−0.365	0.0214
Laggar falcon			
Measured	2.82	−0.433	0.0252
Theoretical	2.74	−0.429	0.0240
Black vulture			
Measured	3.46	−0.430	0.0194
Theoretical	3.48	−0.487	0.0234

* Values for parabolic curves of the form:

$$V_s = a_0 + a_1 V + a_2 V^2$$

are fitted by least squares to measured data and theoretical data calculated from the maximum performance model and the polar curve for minimum drag given by equation 21.

predicted wing span (Fig. 13). Given a PCMD, the model balances the savings in induced drag from extending the wings against the cost in profile drag from increasing the wing area. If the PCMD is too far to the left, the model underestimates the profile drag and finds a wing span that is too large. In fact, the

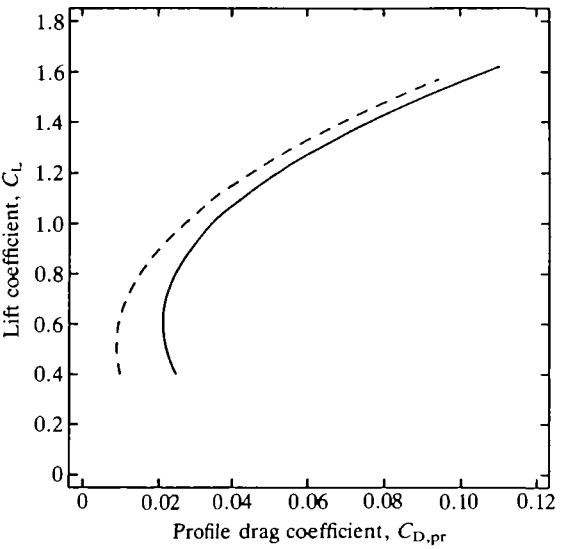

Fig. 11. Polar curves for minimum drag for a gliding Harris' hawk, computed from two different body drag coefficients. Dashed curve uses a value for $S_{fp,B}$ of 0.00264 m^2 calculated from equation 11, and solid curve uses a value for $S_{fp,B}$ of 0.00120 m^2 estimated from measurements in Tucker (1990).

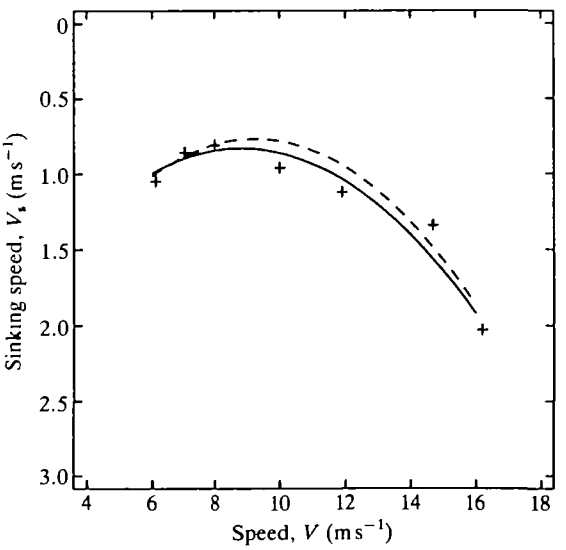

Fig. 12. Theoretical maximum performance curves for a gliding Harris' hawk calculated from the polar curves in Fig. 11. The dashed and solid curves are for $S_{fp,B}$ values of 0.00264 and 0.00120 m^2, respectively. Mean measured points are marked with +.

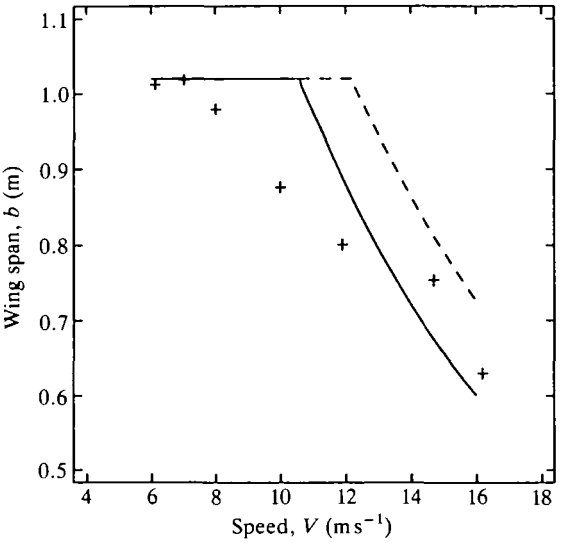

Fig. 13. Theoretical wing spans during maximium performance for the gliding Harris' hawk, calculated from the polar curves in Fig. 11. The dashed and solid curves are for $S_{fp,B}$ values of 0.00264 and 0.00120 m^2, respectively. Mean measured points are marked with +.

model predicts wing spans from equation 20 that are larger than those observed in the hawk at some speeds (Fig. 13). The model also predicts wing spans that are too high for the falcon, although not for the vulture (Tucker, 1987).

In addition, a bird flying in a wind tunnel may keep its wings flexed to avoid collisions with the walls. For example, the hawk with fully spread wings flew within one-quarter wing span of the walls and roof of the working section. At a speed of 10 $m\,s^{-1}$, the hawk moves this distance through the air in about 0.025 s. Flexing the wings reduces the chances of a collision in two ways: it increases the distance between the wing tip and the wall, and it reduces the forces that could accelerate the bird and cause a collision.

When more data for body drag are available, the PCMD given by Tucker (1987) and that given by equation 21 should be recalculated. Until then, they are useful for predicting maximum performance, but equation 22 probably gives a more realistic estimate of the profile drag coefficients of Harris' hawk wings.

This study was partly supported by a Cooperative Agreement (14-16-0009-87-991) between Mark Fuller, US Fish and Wildlife Service and Duke University. We thank Mr F. Presley for loaning the Harris' hawk.

List of symbols

$a_0, \ldots, a_2$ coefficients for maximum gliding performance
b wing span

b_{max}	maximum wing span
C	cross-sectional area of wind tunnel
$C_0, \ldots, C_3$	constants (from Tucker, 1987)
C_D	drag coefficient
$C_{D,pr}$	profile drag coefficient
C_L	lift coefficient
c'	mean chord of wings at maximum span
D	total drag on a bird
D_i	induced drag
D_{par}	parasite drag
$D_{par,B}$	minimum drag of a wingless body at a given speed
D_{pr}	profile drag
d	reference length for Reynolds number
F	correction factor for Reynolds number
k	induced drag factor
k_3, k_4, k_6	constants (from Tucker, 1987)
L	lift
M	mean value of repeated measurements
m	body mass
N	sample size
q	dynamic pressure
Re	Reynolds number
S	wing area
S_{fp}	equivalent flat plate area
$S_{fp,B}$	equivalent flat plate area of a wingless bird body
$S_{fp,r}$	equivalent flat plate area of residual drag
S_{max}	maximum wing area
V	air speed
V_s	sinking speed
W	weight
β	angle between a perpendicular to axis of the camera lens and the plane of the wings
μ	viscosity of air
π	ratio of circumference to diameter of a circle
ρ	air density
θ	glide angle

References

BEDNARZ, J. C. (1988). Cooperative hunting in Harris' hawks (*Parabuteo cinctus*). *Science* **239**, 1525–1527.

CLARK, W. S. (1987). *A Field Guide to the Hawks: North America*. Boston: Houghton Mifflin.

EISENHART, C. (1968). Expression of uncertainties in final results. *Science* **160**, 1201–1204.

GORLIN, S. M. AND SLEZINGER, I. I. (1966). *Wind Tunnels and Their Intrumentation*. Jerusalem, Israel: Israel Program for Scientific Translations.

HOERNER, S. F. (1965). *Fluid-dynamic Drag*. Brick Town, NJ: S. F. Hoerner.

KU, H. H. (1969). Notes on the use of propagation of error formulas. *J. Research natn. Bureau of Standards* **70**C, 263–273.

PARROT, C. G. (1970). Aerodynamics of gliding flight of a black vulture *Coragyps atratus*. *J. exp. Biol.* **53**, 363–374.

PENNYCUICK, C. J. (1968). A wind-tunnel study of gliding flight in the pigeon *Columba livia*. *J. exp. Biol.* **49**, 509–526.

PENNYCUICK, C. J. (1971). Control of gliding angle in a Rüppell's griffon vulture *Gyps rüppellii*. *J. exp. Biol.* **55**, 39–46.

PENNYCUICK, C. J. (1975). Mechanics of flight. In *Avian Biology*, vol. V (ed. D. S. Farner and J. R. King), pp. 1–75. New York: Academic Press.

PENNYCUICK, C. J. (1989). *Bird Flight Performance: a Practical Calculation Manual*. Oxford: Oxford University Press.

POPE, A. AND HARPER, J. J. (1966). *Lowspeed Wind Tunnel Testing*. New York: Wiley & Sons.

SNEDECOR, G. W. AND COCHRAN, W. G. (1980). *Statistical Methods*. Ames: Iowa State University.

TUCKER, V. A. (1973). Bird metabolism during flight: evaluation of a theory. *J. exp. Biol.* **58**, 689–709.

TUCKER, V. A. (1987). Gliding birds: the effect of variable wing span. *J. exp. Biol.* **133**, 33–58.

TUCKER, V. A. (1988). Gliding birds: descending flight of the white-backed vulture, *Gyps africanus*. *J. exp. Biol.* **140**, 325–344.

TUCKER, V. A. (1990). Body drag, feather drag and interference drag of the mounting strut in a peregrine falcon, *Falco peregrinus*. *J. exp. Biol.* **149**, 449–468.

TUCKER, V. A. AND PARROTT, C. G. (1970). Aerodynamics of gliding flight in a falcon and other birds. *J. exp. Biol.* **52**, 345–367.

VON MISES, R. (1959). *Theory of Flight*. New York: Dover Publications.